THE TELFONA PATHFINDER WING FOR THE CALIBRATION OF THE ETW WIND TUNNEL

G. Schrauf
Airbus
Airbus Allee 1
28199 Bremen, Germany

K. H. Horstmann, T. Streit
DLR
Lilienthalplatz 7
38108 Braunschweig, Germany

ABSTRACT

The e^N-method, based on linear stability theory, is currently the most sophisticated method used for transition prediction in engineering applications. Being a semi-empirical method, it needs to be calibrated for each wind tunnel and also for free flight conditions. In this paper, we describe the design of a wing which will be used for the calibration of the European Transonic Windtunnel (ETW) within the European TELFONA project.

1. INTRODUCTION

The prediction of the laminar-turbulent transition in a boundary layer is of utmost importance for engineering applications in aviation. Many efforts have been undertaken to tackle this task. Transition prediction tools range from those based on simple criteria, using only a few boundary layer parameters, to very sophisticated methods computing the non-linear growth and interaction of the instabilities in the boundary layer. Yet neither extreme of this range is suitable for today's engineering applications. On the one hand, using simple criteria lacks accuracy. On the other hand, non-linear calculations, though increasingly feasible with today's computers, cannot be used because we do not know initial amplitudes. Linear methods, such as e^N-methods based on the computation of growth rates of characteristic disturbances represent a usable alternative for engineering purposes. These methods require no knowledge of initial amplitudes.
The e^N-methods' disadvantage, meanwhile, is that they can only be used in a semi-empirical way. To be able to predict transition, we need to calibrate the method with transition measurements in similar situations. Due to the differences in background turbulence and noise, such calibration measurements have to be performed for each wind tunnel as well as for free flight. A lot of expertise has been obtained in previous programmes[1], however, an N-factor calibration for the ETW wind tunnel is still missing. This gap will be filled by the TELFONA programme, in which the tests with the so-called PATHFINDER wing will provide such a calibration. In this paper, we report on the design of this calibration wing.

2. SPECIFICATIONS FOR THE DESIGN OF THE PATHFINDER WING

The PATHFINDER wing is to be tested at Mach and Reynolds numbers relevant for current transport aircraft. Because the wing is designed for calibration, transition should occur far enough from the leading edge to be easily detectable by infrared photometry. Thus, we require transition to occur between 30% and 50% chord on upper or lower side where the wing curvature is relatively small.

To obtain laminar flow up to those chordwise positions, the leading edge sweep must be chosen to avoid attachment line contamination. A sweep and Reynolds number range for which natural laminar flow was previously obtained is given in Figure 2 of [2]. Among the tests presented in this figure, the one with the Fokker F100 aircraft performed in the European ELFIN programme[3,4,5] provided us with guidelines for our choices. In these flight tests, laminar flow was achieved for Mach numbers between 0.5 and 0.8 and Reynolds numbers from 17 to 30 million (cf. [2, Table 1]). With this in mind, we chose target Mach numbers around 0.78 ± 0.02 and sweep angles of $18^O \pm 4^O$. Due to the size of the measuring section of the ETW, the wingspan is limited to 1.8 m and the chord length cannot exceed 0.25 m. Because with today's infra-red cameras the most sensitive temperatures for infrared transition detection in a cryogenic tunnel are around 180^OK, we obtain Reynolds numbers in the order of 20 million. No restriction was imposed on the lift coefficient in the design phase.
The different instability modes can exhibit non-linear interactions in the boundary layer, which are not taken into account by the linear e^N-method. Therefore, we aim for cases with clear Tollmien-Schlichting as well as with clear cross-flow transitions to be realized by a variation of sweep and angle of attack.
For the design we have to assume an N-factor range, even though we have yet to calibrate the ETW tunnel. Based on previous experience with local, incompressible instability theory, we estimate that Tollmien-Schlichting N-factors will fall in the range between 6 and 10 and cross-flow N-factors between 5 and 8 if computed with the code suite and the numerical settings used in [1]. The N-factor range might be different for other codes and different numerical settings. To obtain good correlations, we require

the pressure distributions on the wing to be such that they generate linear N-factor envelopes with moderate gradients in the above range. A steep gradient makes transition prediction easy. However, small inaccuracies in the determination of the transition location will result in a large variation for the correlated N-factor, so that a steep gradient is not suitable for correlation.
Another point is that we cannot measure pressure and transition at the same location on the wing, because the pressure taps cause turbulent wedges. Therefore, we aim for a wing with weak taper (a taper ratio of 7/9 is proposed), no dihedral, and parallel isobars (at least between 30% and 70% span) on upper as well as on lower side. This allows us to get the pressure information with only two sections of pressure taps and to have a region with undisturbed flow in between. An additional advantage of weak taper is that it allows for the evaluation with non-local PSE methods, which are currently only developed for infinitely long, swept wings.

3. DESIGN OF THE 2-D AIRFOIL

Based on the above specifications, several airfoils were designed by CIRA, DLR and ONERA with 2.5D-methods.

CIRA designed two candidate airfoils[6] using a genetic algorithm driving an Euler-boundary-layer method with an implemented data base method for transition prediction[7]. The objective function was chosen to obtain linear envelopes for Tollmien-Schlichting and also for cross-flow N-factors within the required ranges. The initial airfoil was based on the ATTAS NLF glove. For the design Mach number, both CIRA airfoils exhibit cross-flow transition before 10% chord on the lower side (cf. Fig. 1). On the upper sides, both airfoils have the desired linear envelope for the N_{TS}-factors. However, the N_{CF}-factors grow rapidly until they reach a plateau at 20% chord. If the level of this plateau is sufficiently low, cross-flow amplification is expected to be weak so that Tollmien-Schlichting waves dominate the transition. This might be the case for the sweep angle of 14^{O} as can be seen from Fig. 2. However, already for 18^{O} sweep, the N_{CF}-factors reach a level close to six at 5% chord, which would result in a mixed Tollmien-Schlichting / cross-flow or a cross-flow dominated transition. For larger sweep angles the N_{CF}-factor plateau reaches a level indicating an early cross-flow transition.
DLR used the DLR LV5 profile as their starting point, and designed an airfoil with an inverse method based on the FLOWer RANS code[8,9]. The transition behaviour was analyzed by Airbus[10]. On its upper side, the airfoil delivers five good cases for CF-correlation (the case with Mach 0.78 and C_l = 0.1 being shown in Fig. 3), five for TS-correlation, and one mixed case. On the lower side, there are three cases for CF-correlation, five for TS-correlation (N_{ST} and N_{CF}-factors for the lower side of the above case with Mach 0.78 and C_l = 0.1 being shown in Fig. 4), and two cases with mixed transition. As with the CIRA airfoil, some effort was needed to obtain good TS-cases for the envisaged sweep angles. Altogether, eight good cases for CF-correlation, ten for TS-correlation, and, three mixed cases were obtained. This constitutes a good number of cases to obtain a useful band of limiting (N_{TS},N_{CF})-factor pairs.
ONERA used an inverse design method coupled with the elsA RANS code and derived an airfoil[11] from the Fokker F100 NLF glove[3] which is discussed in [6]. The objective was to obtain linear envelopes of Tollmien-Schlichting and cross-flow N-factors on the upper and lower sides of the airfoil, but not necessarily for the same aerodynamic conditions. Typical results are shown, for Mach number 0.78 and sweep angle 18^{O} in Fig. 5 for the upper side with an incidence angle of -1^{O} and in Fig. 6 for the lower side with incidence $+1^{O}$. On the upper side, the airfoil has a cross-flow transition before 10% chord. The lower side becomes a good TS-case angle if the sweep angle is reduced to 14^{O} because the cross-flow N-factors reach only the level of four. However, with 18^{O} sweep, the cross-flow amplification is already too strong and produces an early CF-transition at approximately 15% chord as can be seen from Fig. 6.
A comparison of all three airfoils is shown in Fig. 7. Even though the CIRA and ONERA designs could have been developed further, the airfoil proposed by DLR was the most developed one at the time at which the selection for the three-dimensional design work needed to be done.

4. DESIGN OF THE 3-D WING

The two-dimensional airfoil was the basis for the design of the three-dimensional wing. An important design objective was the requirement of parallel isobars over a large part of the wing, at least between 30% and 70% of the span. Moreover, the wing was to be mounted to an existing fuselage model, so that the presence of the fuselage had to be taken into account. Based on the requirements of having no dihedral, a taper ratio of 7/9, and assuming a span of 1.7 m, we obtain the plan form shown in Fig. 8.

First, a 3D wing alone design was performed with this planform. Using the C_P distribution of the DLR airfoil as target for all wing sections, we got an initial twist distribution for the wing body configuration with an inverse design method. To obtain a pressure distribution close to the target, large geometry changes were required at the wing tip resulting in increased thickness and increased twist.
In the second step, the wing had to be fitted to the existing fuselage with a suitable belly fairing. First calculations indicated that the isobar target could not be reached close to the fuselage, because its presence lead to a different wing trailing edge pressure level, which varies from tip to root as shown in Fig. 9. To obtain constant trailing edge pressure, the target pressure distribution was modified. The result is shown in Fig. 10, spanwise twist and thickness are presented in Fig. 11. Note that in contrast to the constant thickness t/c=0.1246 of the initial geometry, the second design has the larger thickness of t/c=0.160 at the root and a smaller thickness of t/c=0.108 at h=0.20. Towards the tip the thickness increases again to larger values. The increased thickness close to the root and to the tip is shown also in Fig. 12 which gives a front view of the initial and second design. Local lift values are given in Fig. 13. Note that between 10% and 70% span an almost constant local lift value is obtained.
In the third step the target pressure distribution was altered to improve the design in the region close to the root section by decreasing the thickness at the root to t/c=0.14 and increasing the minimum thickness to t/c=0.11 to obtain a smoother twist distribution at the root. The resulting pressure distributions are given in Fig. 14. Compared to the previous design step, the pressure distributions are now closer to the target, also for the sections close to the root. The spanwise twist and thickness and local lift values for the obtained geometry

are presented in Fig. 15.
The surface pressure contours are given in Fig. 16 for the lower surface and in Fig. 17 for the upper surface. The wing has a spanwise constant sectional pressure distribution with parallel isobars between 30% and 70% span, which was one of the design requirements. Parallel isobars are obtained also beyond this region, especially on the lower surface.

5. ANALYSIS OF THE DESIGN

For the analysis of the design, 3D RANS solutions were obtained for the pathfinder wing for the design Mach numbers M=0.78 and also for the Mach numbers M=0.76 and M=0.80. The computations were done for the design lift coefficient C_l = 0.216 as well as for C_l = 0.1 and for C_l = 0.334 taking the three sweep angles of 14^O, 18^O, and 22^O into account. Altogether fourteen 3D solutions were considered for further analysis with linear stability theory. For each solution we considered the lower and upper side of the wing at the three spanwise sections h =0.36, 52, 66. Altogether we considered seventy-eight boundary layers and analysed their stability[10]. The results show that the three-dimensional wing has indeed the stability properties of the two-dimensional airfoil. Furthermore, the isobar concept results in an N-factor growth that is nearly independent of the spanwise location.

An overview of the expected transition properties of all cases considered is given in Figs. 18-20. In these figures abbreviation “TS” represents a Tollmien-Schlichting dominated transition, “CF” a crossflow dominated one and “MIXED” stands for a transition with large TS as well as large CF amplification so that both instabilities will play a significant role. Cases that are well suited for correlation are in green, black indicates a case which is still usable, and red one that is unusable for correlation. An example of such a case is given in Fig. 21 (sweep 14^O, Ma = 0.78, C_l = 0.216). We observe a large extent of laminar flow which is bounded by a Tollmien-Schlichting transition at 55% chord. This would be an excellent case if we aimed for laminar flow. The transition location is also easy to predict. However, for correlation this case is less suitable because the gradient of the envelope of the N_{TS}-factors is too steep.

ACKNOWLEGDEMENT

This work is performed within the TELFONA project (www.telfona.com; contract number 516109) supported by the European Commission in Framework Programme 6. We especially thank Anne-Marie Rodde and Jean-Luc Godard, ONERA, as well as Raffaele Donelli and Domenico Quagliarella, CIRA, for their design contributions.

REFERENCES

[1] G. Schrauf,
Large-Scale Laminar-Flow Tests Evaluated with Linear Stability Theory, AIAA Journal of Aircraft, Vol. 41, No. 2, March-April 2004, pp. 224 - 230.

[2] G. Schrauf,
Status and Perspectives of Laminar Flow, The Aeronautical Journal, December 2005, Vol. 109, No. 102, pp. 639-644.

[3] U. Dreßler, H. Hansen, S. Rill, K.H. Horstmann, C.H. Rohardt, G. Wichmann,
Design of the Fokker 100 Natural Flow Glove, ELFIN Technical Report No. 7, 5th March 1992.

[4] H. Hansen, G. Schrauf, R. Rohard,
Erste Ergebnisse der F100 Laminarhandschuhtests. In: Strömungen mit Ablösung, 8. DGLR Fach-Symposium 10.-12. November 1992, Köln-Porz. DGLR-Bericht 92-07, 1992.

[5] G. Schrauf, J. Perraud, F. Vitello, F. Lam, H. W. Stock, A. Abbas,
Transition Prediction with Linear Stability Theory - Lessons Learned from the ELFIN F100 Flight Demonstrator. 2nd European Forum on Laminar Flow Technology, 10.-12. 6. 1996, Bordeaux. Proceedings published by AAAF, 6, Rue Galilée, 75782 Paris, France

[6] D. Quagliarella,
TELFONA Task 1.1 on 2.5D Airfoil Design and Analysis for use in Pathfinder Wing, TELFONA Technical Report CIRA-TR-05-0337, May 2006.

[7] R. S. Donelli, G. Casalis,
Database Approach – Stationary Mode Treatment, ALTTA Technical Report ALTTA-CIRA-TR-AEP-01-039, April 2001.

[8] Th. Streit, K. H. Horstmann,
NLF pathfinder wing design and evaluation at ETW test points, TELFONA Technical Report D1.1-4, November 2006.

[9] W. Bartelheimer,
Ein Entwurfsverfahren für Tragflügel in transsonischer Strömung, Dissertation TU-Braunschweig,
DLR FB 96-30,1996.

[10] G. Schrauf, K. Schmidt,
Prediction of the Transition Behaviour of the TELFONA pathfinder wing, TELFONA Technical Report D1.1-5, November 2006.

[11] J.-L. Godard,
TELFONA Deliverable D1.1-2- Wing Section Data, Technical Report, December 2005.

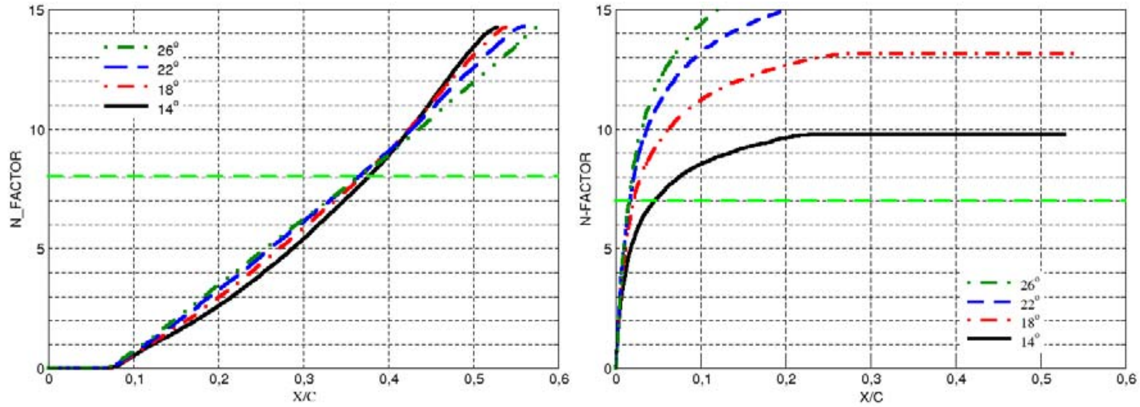

FIGURE 1: Variation of Tollmien-Schlichting N-factors (left) and cross-flow N-factors (right) with sweep angle for the lower side of CIRA airfoil 1.

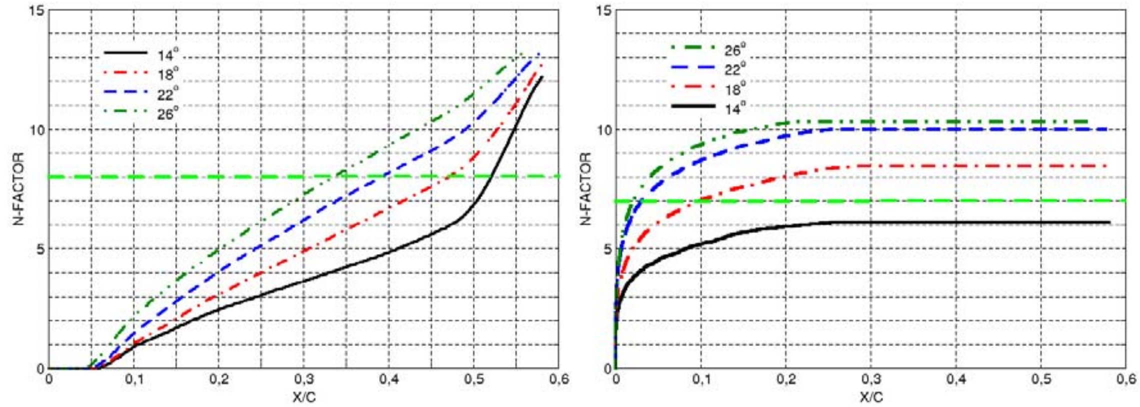

FIGURE 2: Variation of Tollmien-Schlichting N-factors (left) and cross-flow N-factors (right) with sweep angle for the upper side of CIRA airfoil 1.

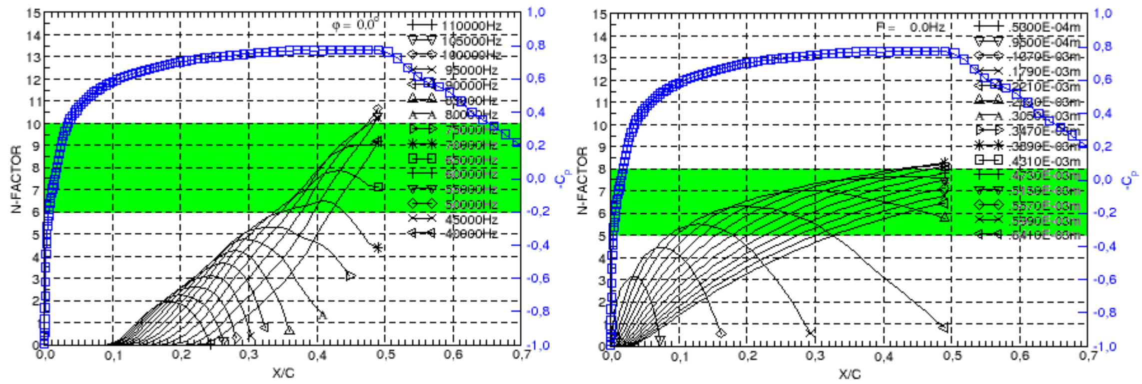

FIGURE 3: Tollmien-Schlichting N-factors (left) and cross-flow N-factors (right) of a cross-flow case for the upper side with the DLR airfoil.

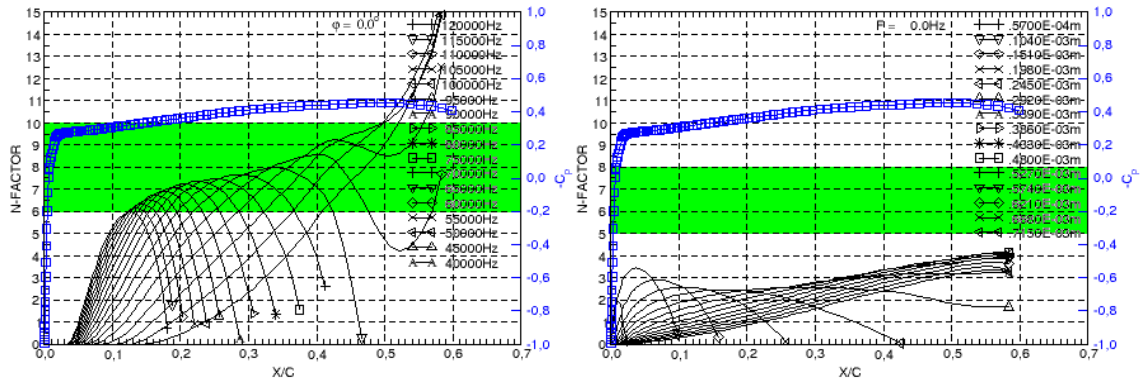

FIGURE 4: Tollmien-Schlichting N-factors (left) and cross-flow N-factors (right) of a Tollnien-Schlichting case for the lower side with the DLR airfoil.

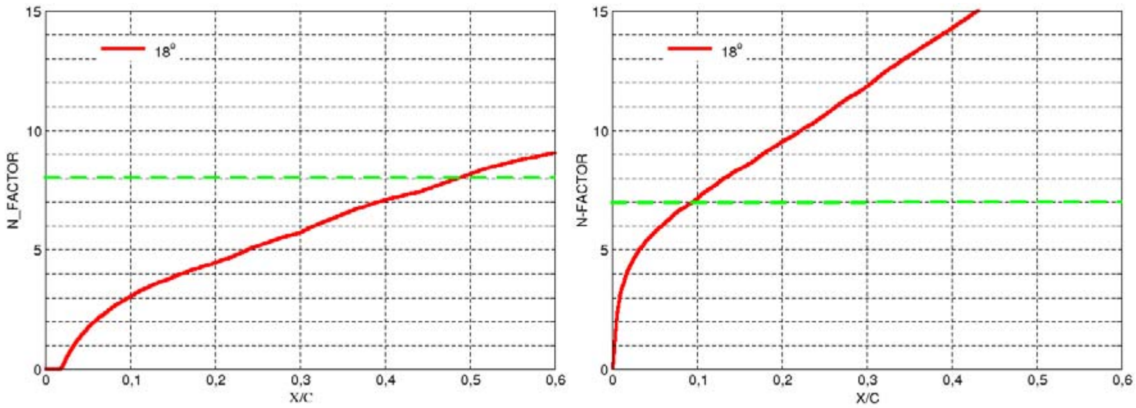

FIGURE 5: Tollmien-Schlichting N-factors (left) and cross-flow N-factors (right) for the upper side of ONERA airfoil with angle of attack -1^0.

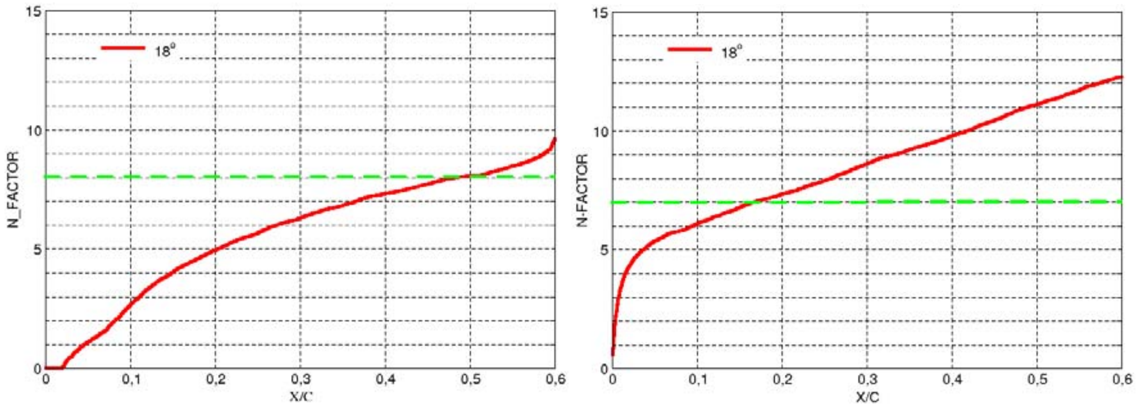

FIGURE 6: Tollmien-Schlichting N-factors (left) and cross-flow N-factors (right) for the lower side of ONERA airfoil with angle of attack $+1^0$.

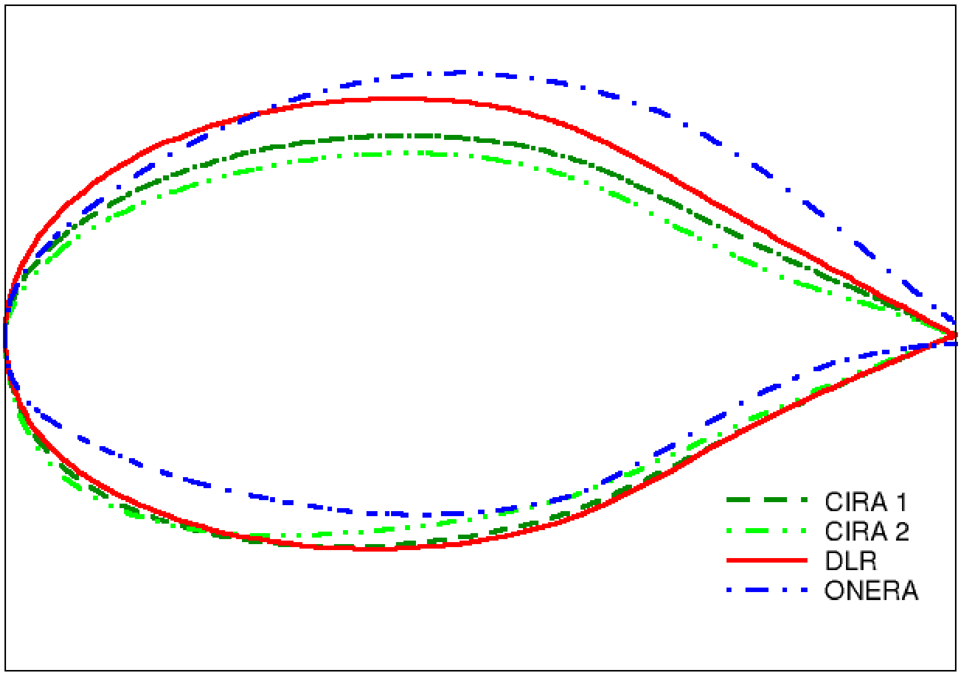

FIGURE 7: Comparison of the airfoils proposed by CIRA, DLR, and ONERA.

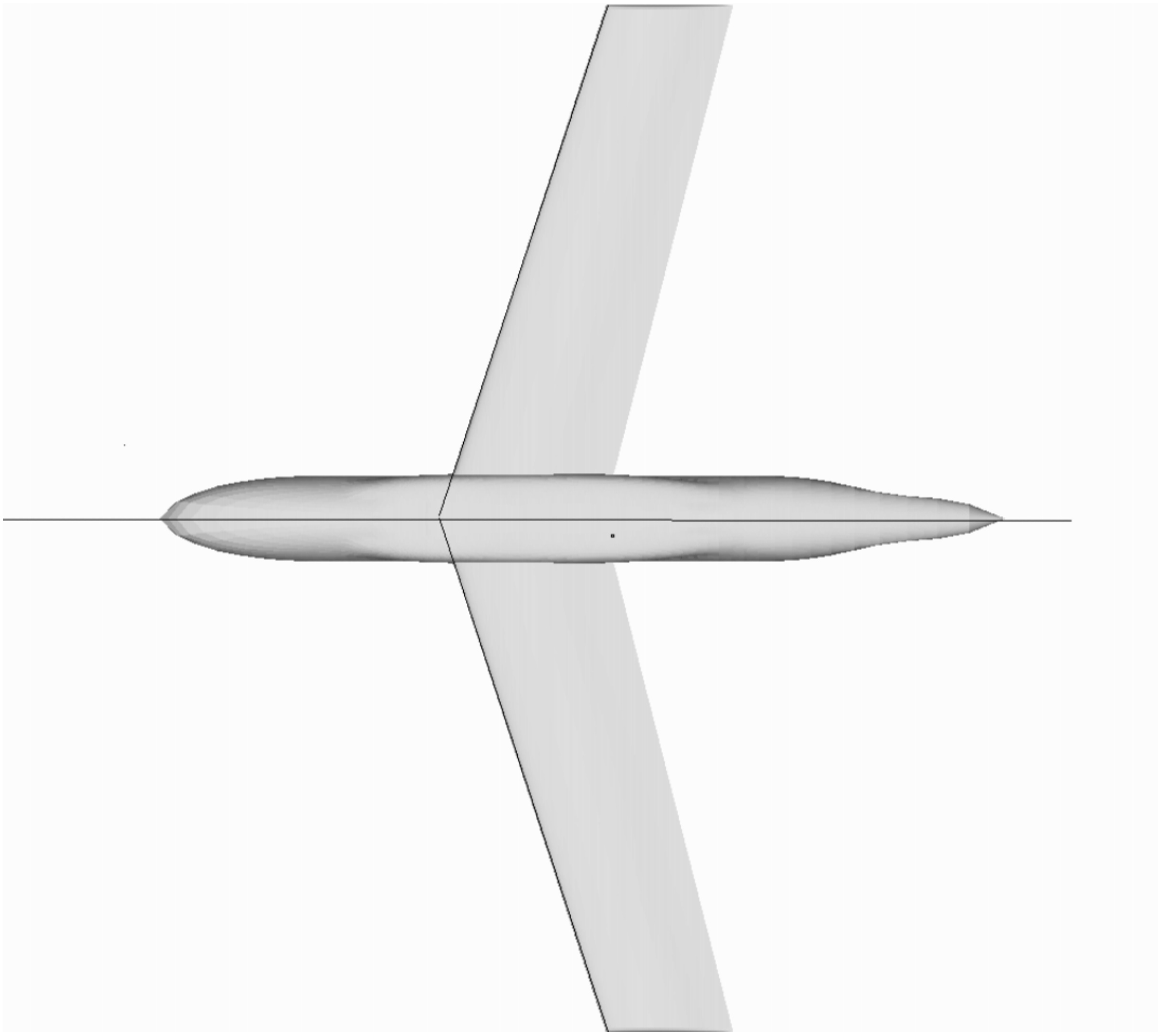

FIGURE 8: Top view of Pathfinder model

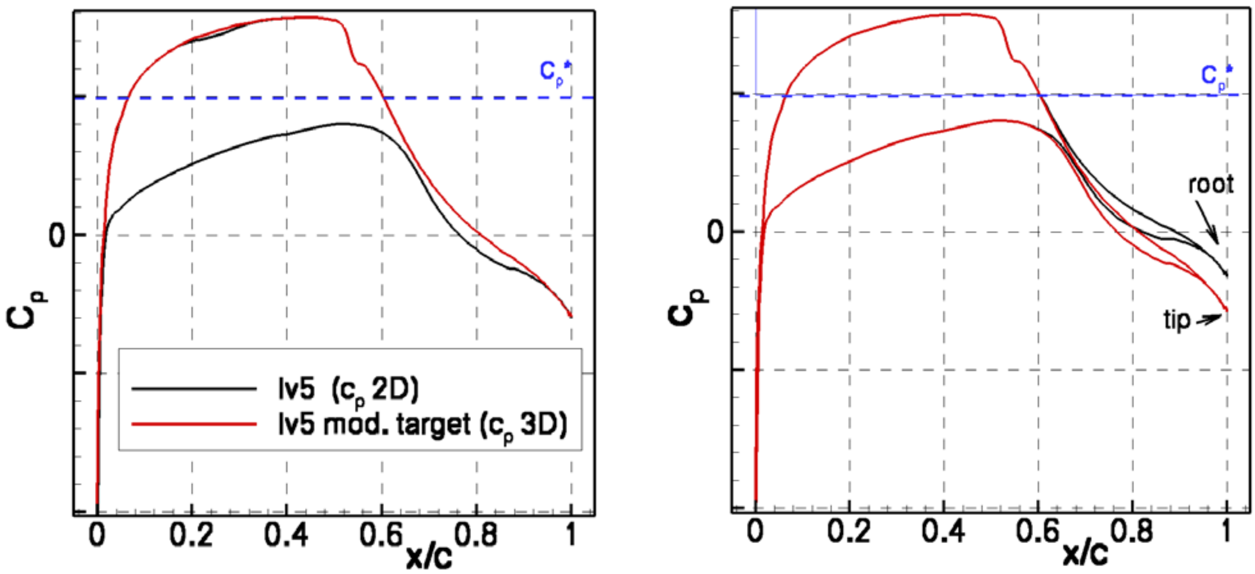

FIGURE 9: Initial Cp distributions.

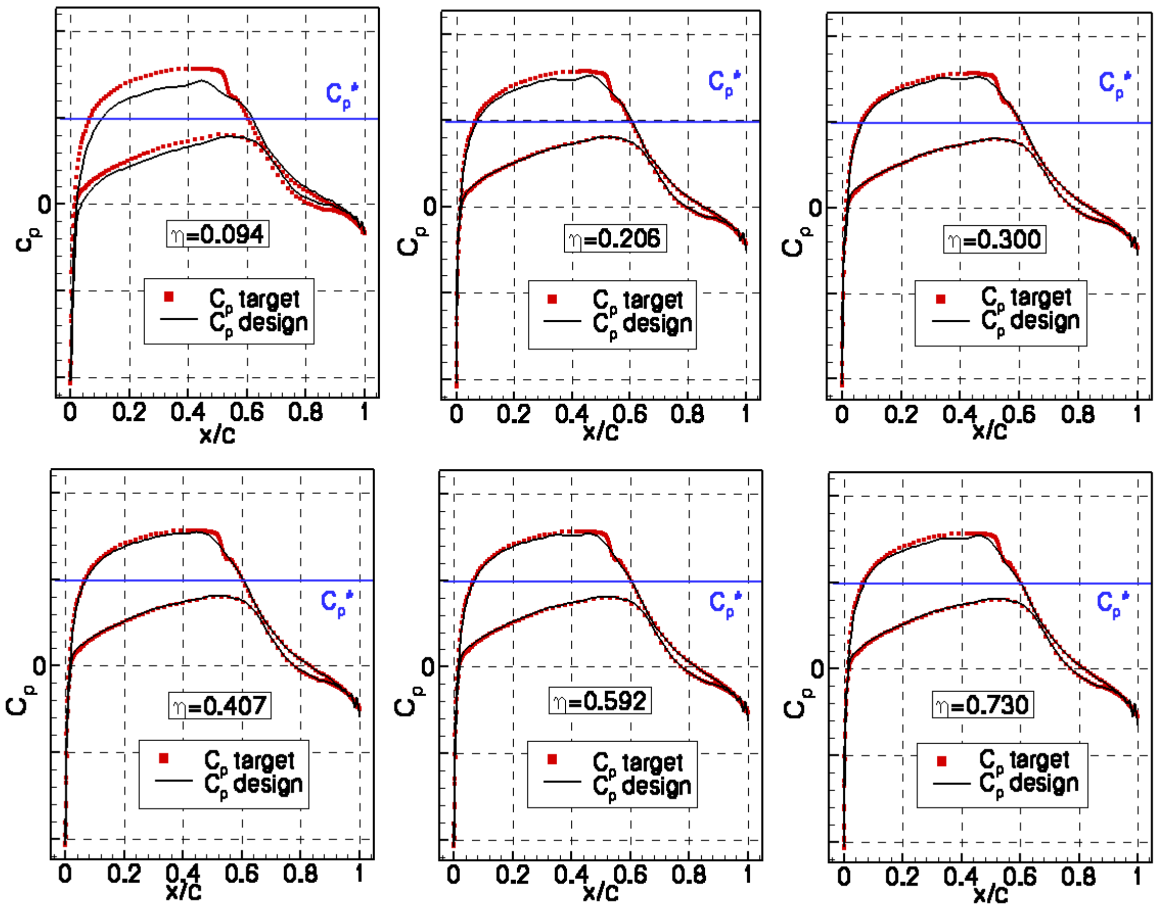

FIGURE 10: Cp distributions of the second design step.

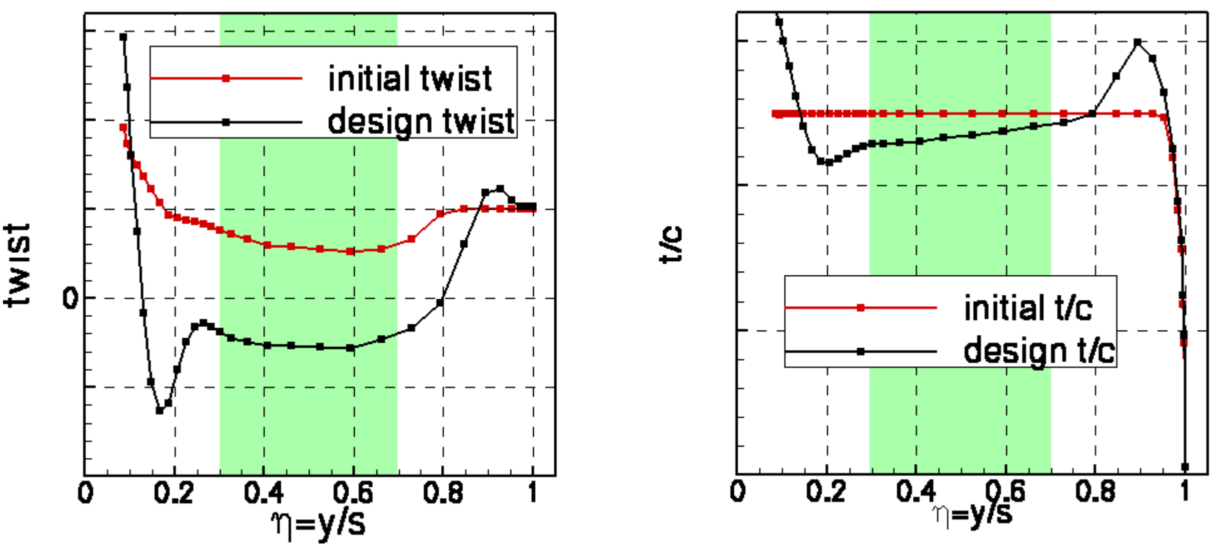

FIGURE 11: Spanwise twist and thickness distribution of the second design step.

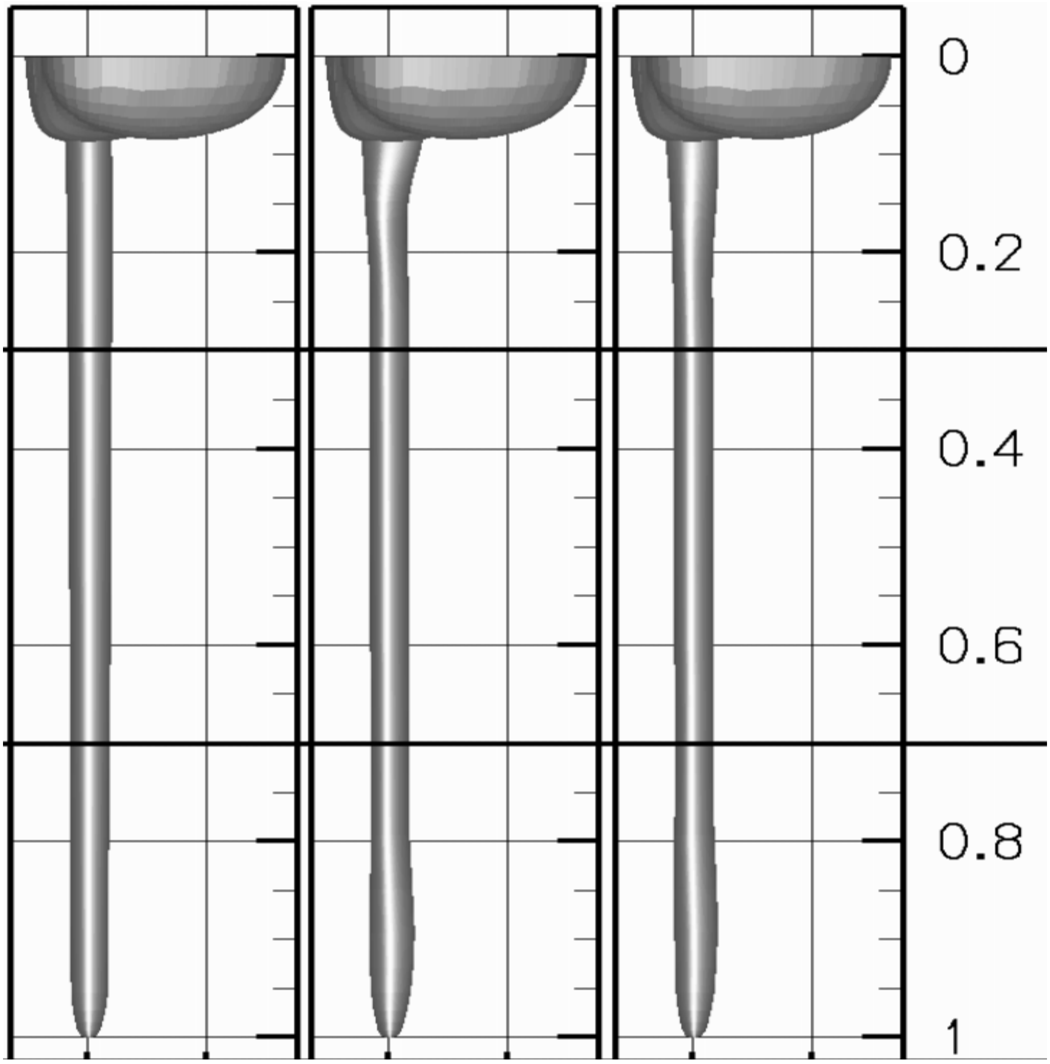

FIGURE 12: Front view of initial, step 2, and final geometry

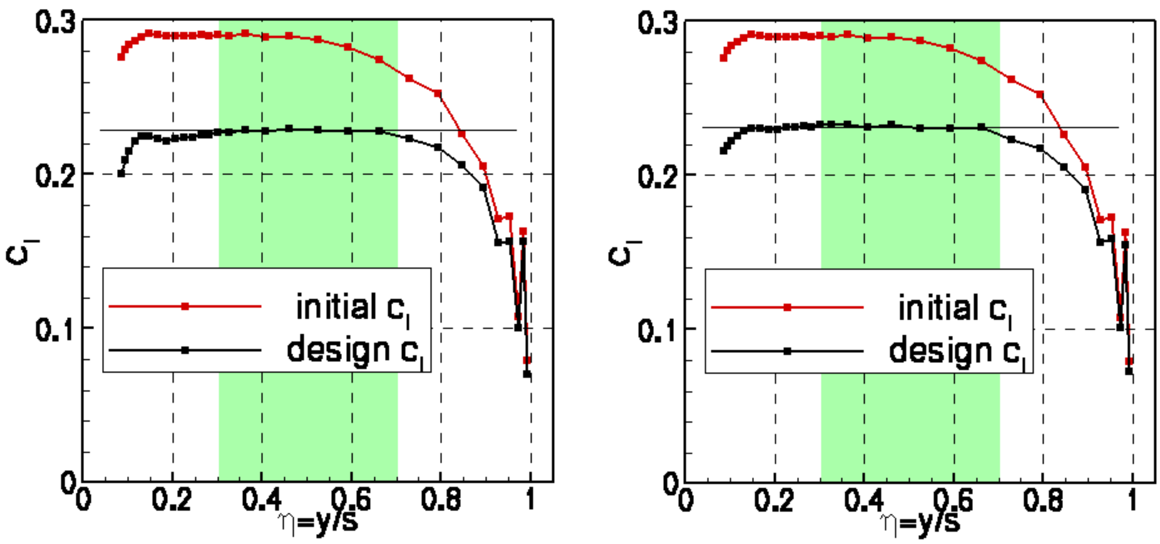

FIGURE 13: Local lift distribution of step 2 and the final step.

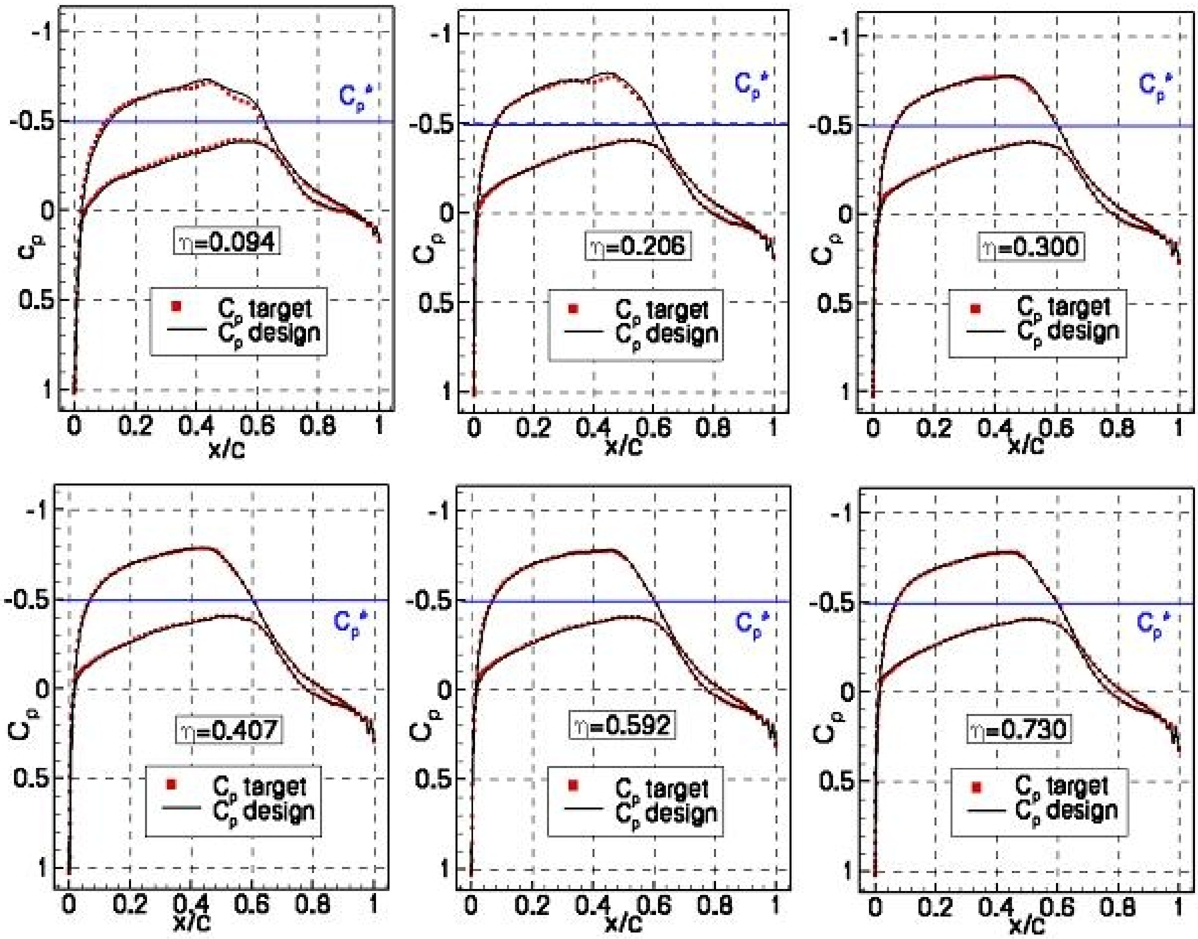

FIGURE 14: Final Cp distributions.

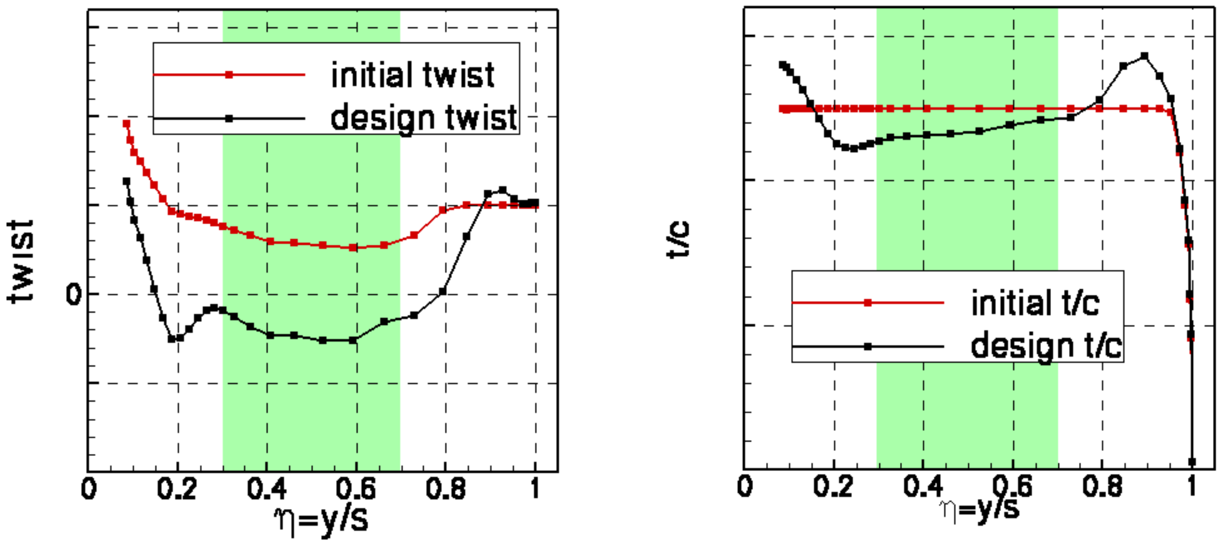

FIGURE 15: Final spanwise twist and thickness distribution.

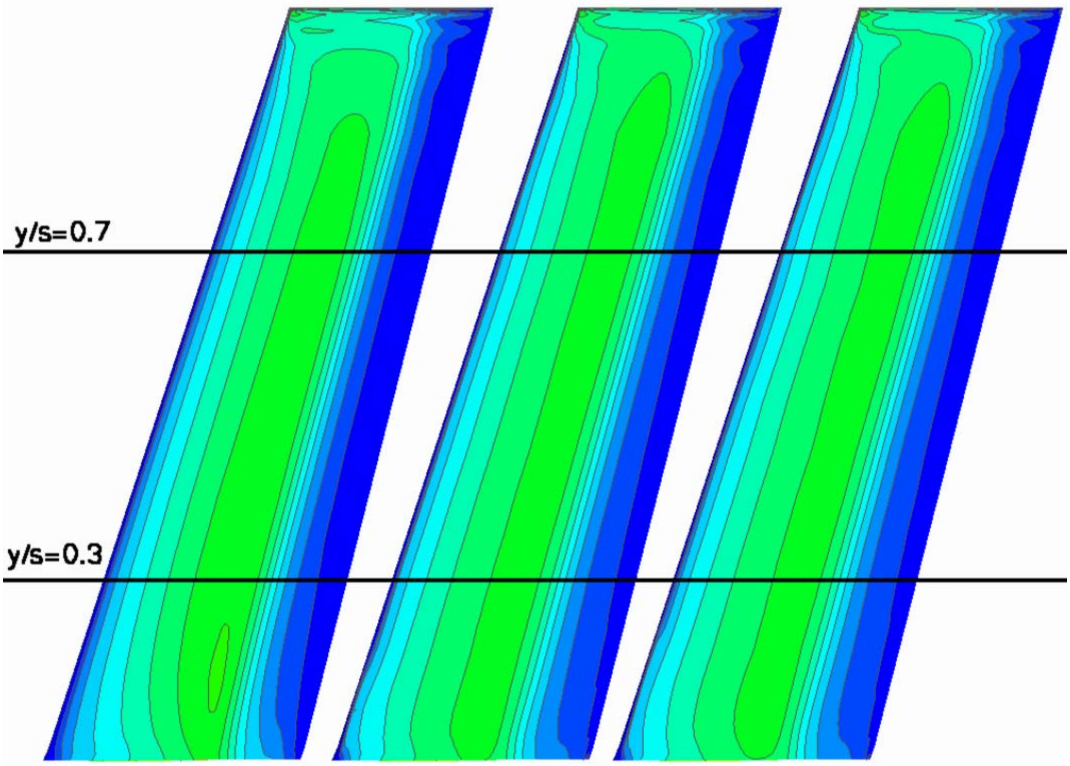

FIGURE 16: Pressure contours on lower surface for initial wing and the second and third design step. M=0.78, Re=20x10^6.

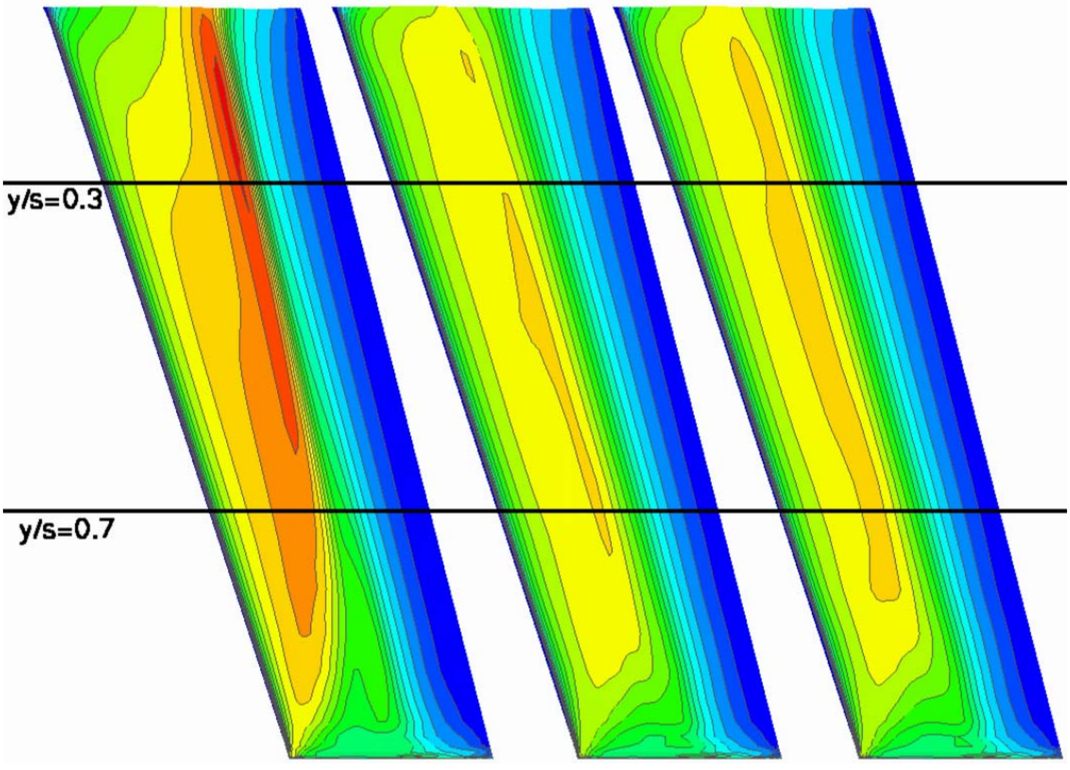

FIGURE 17: Pressure contours for upper surface for initial wing and the second and third design step. M=0.78, Re=20x10^6.

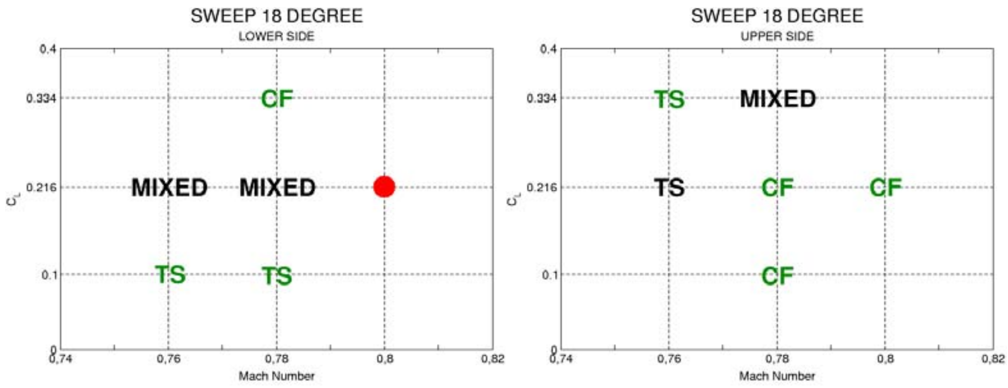

FIGURE 18: Expected transition scenarios for 18 degree sweep.

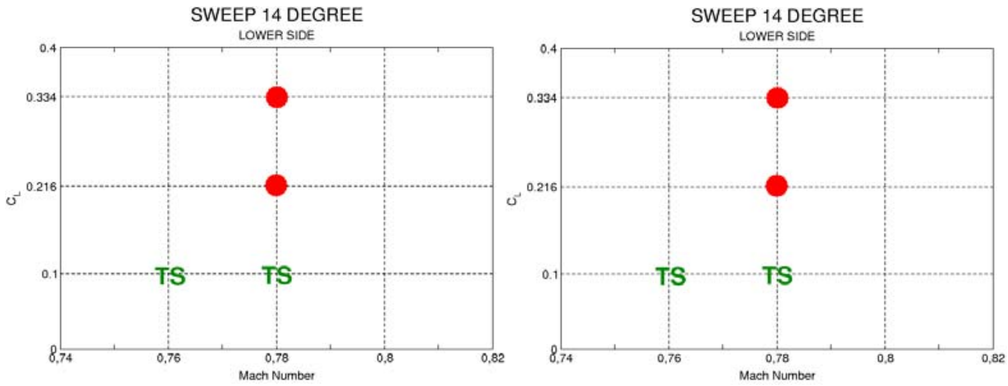

FIGURE 19: Expected transition scenarios with reduced sweep of 14 degree.

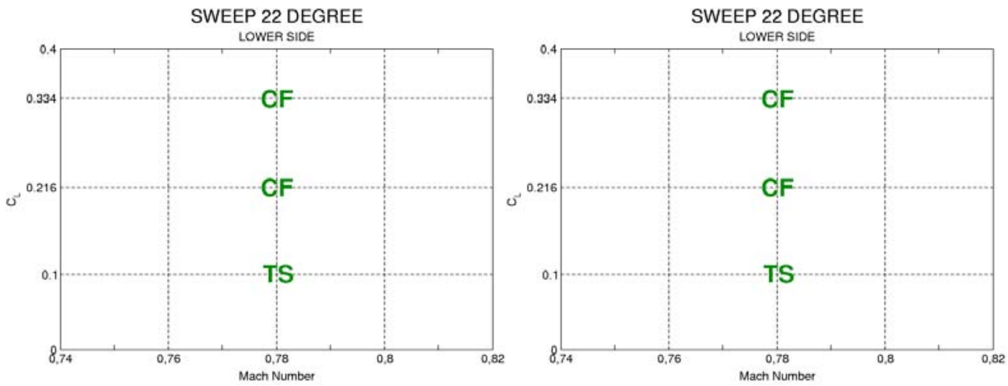

FIGURE 20: Expected transition scenarios with increased sweep of 22 degree.

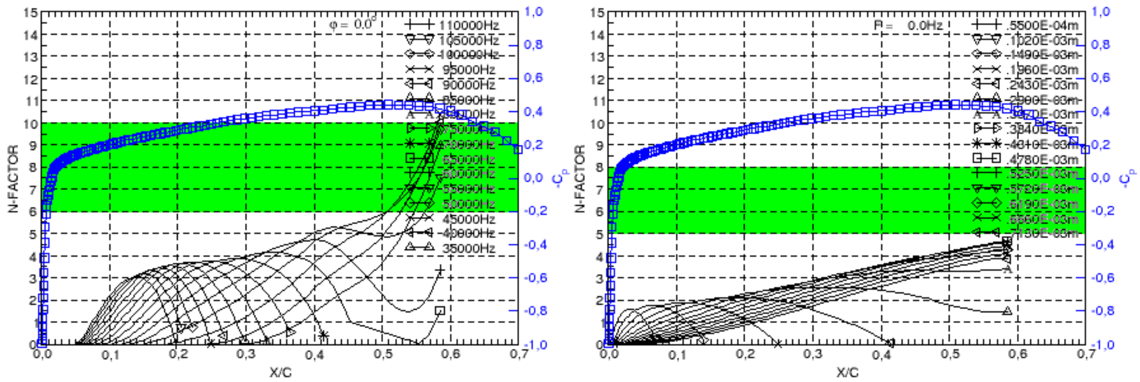

FIGURE 21: Tollmien-Schlichting N-factors (left) and cross-flow N-factors (right) of a case that is unsuitable for correlation.